

1-Methyl-4-phenyl-1,2,3,6-tetrahydropyridine as a Substrate of Cytochrome P450 2D6: Allosteric Effects of NADPH–Cytochrome P450 Reductase[†]

S. Modi,^{‡,§} D. E. Gilham,^{||} M. J. Sutcliffe,[⊥] L.-Y. Lian,[§] W. U. Primrose,[§] C. R. Wolf,^{||} and G. C. K. Roberts^{*,‡,§}

Centre for Mechanisms of Human Toxicity, Departments of Biochemistry and Chemistry, and Biological NMR Centre, University of Leicester, Leicester LE1 9HN, U.K., and Biomedical Research Centre, Ninewells Hospital and Medical School, University of Dundee, Dundee DD1 9SY, U.K.

Received October 21, 1996; Revised Manuscript Received December 31, 1996[®]

ABSTRACT: 1-Methyl-4-phenyl-1,2,3,6-tetrahydropyridine (MPTP), a neurotoxin that produces Parkinsonism symptoms in man, has been examined as a substrate of recombinant human cytochrome P450 2D6. When cumene hydroperoxide is used as an oxygen and electron donor, a single product is formed, identified as 4-phenyl-1,2,3,6-tetrahydropyridine. The K_m for formation of this product (130 μ M) is in agreement with the dissociation constants for MPTP binding to the enzyme determined by optical and nuclear magnetic resonance (NMR) spectroscopy. When the reaction is carried out with nicotinamide adenine dinucleotide phosphate (reduced) (NADPH) and recombinant human NADPH–cytochrome P450 reductase, a second product, identified as 1-methyl-4-(4'-hydroxyphenyl)-1,2,3,6-tetrahydropyridine, is formed in addition to 4-phenyl-1,2,3,6-tetrahydropyridine. The K_m values for formation of these two products are 19 μ M and 120 μ M, respectively. Paramagnetic relaxation experiments have been used to measure distances between the protons of bound MPTP and the heme iron, and these have been used to construct models for the position and orientation of MPTP in the active site. For the cytochrome alone, a single mode of binding was observed, with the N-methyl close to the heme iron in a position appropriate for the observed N-demethylation reaction. In the presence of the reductase, the data were not consistent with a single mode of binding but could be explained by the existence of two alternative orientations of MPTP in the active site. One of these, characterized by a dissociation constant of 150 μ M, is essentially identical to that observed in the absence of the reductase. In the second, which has a K_d of 25 μ M, the MPTP is oriented so that the aromatic ring is close to the heme iron, in a position appropriate for *p*-hydroxylation leading to the formation of the product seen only in the presence of the reductase. In the case of codeine, another substrate for cytochrome P450 2D6, the addition of reductase had no effect on the nature of the product formed, the dissociation constant, or the orientation in the binding site. These observations show that NADPH–cytochrome P450 reductase has an allosteric effect on the active site of cytochrome P450 2D6 that affects the binding of some substrates but not others.

The cytochrome P450s catalyze the monooxygenation of a wide variety of compounds through the insertion of one atom of molecular oxygen into the substrate, with the concomitant reduction of the other atom to water. The members of this family that occur in the endoplasmic reticulum of mammals play a central role in determining the response of the organisms to foreign chemicals, both therapeutic drugs and environmental contaminants. Among these, cytochrome P450 2D6 (CYP 2D6)¹ metabolizes a wide range of compounds containing a basic nitrogen atom

(Eichelbaum & Gross, 1990; Tucker, 1994), including a number of clinically important drugs. It is responsible for the so-called debrisoquine/sparteine-type polymorphism (Lenard, 1990; Meyer *et al.*, 1990; Kroemer & Eichelbaum, 1995; Bertilsson, 1995) which occurs in ~7% of the Caucasian population. This polymorphism has been associated with adverse, and in certain instances life-threatening, drug side effects due to differences in metabolism (*e.g.*, Price-Evans *et al.*, 1980). The commonest genetic defect at the CYP 2D6 locus in Caucasian populations arises from aberrant splicing, resulting in the introduction of a stop codon and the absence of CYP 2D6 protein (Gough *et al.*, 1990; Kroemer & Eichelbaum, 1995; Bertilsson, 1995). In Oriental populations, on the other hand, this mutant allele is almost absent, but as many as 50% of the population have a single amino acid substitution (Pro34 → Ser) which leads to lower activity of the enzyme (Bertilsson, 1995).

There is a 2.5-fold greater incidence of the CYP 2D6 “poor metabolizer” genotype in patients with Parkinson’s disease compared to controls (Tanner, 1991; Smith *et al.*, 1992), suggesting that the activity of CYP 2D6 may be a significant factor in the susceptibility to Parkinson’s disease [see Gilham *et al.* (1997)]. This could be understood if a neurotoxin

[†] This work was supported by a grant, and a studentship to D.E.G., from the Medical Research Council. M.J.S. is a Royal Society University Research Fellow.

* Address correspondence to this author at the Centre for Mechanisms of Human Toxicity, University of Leicester, P.O. Box 138, Hodgkin Building, Lancaster Rd., Leicester LE1 9HN, U.K. Telephone +44-116-252-5534; Fax +44-116-252-5616.

[‡] Centre for Mechanisms of Human Toxicity, University of Leicester.

[§] Department of Biochemistry and Biological NMR Centre, University of Leicester.

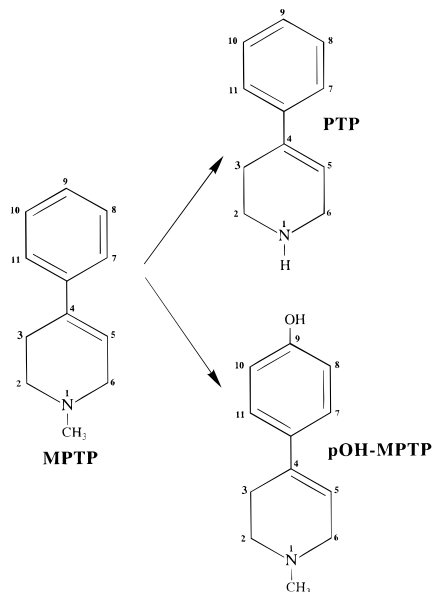
^{||} University of Dundee.

[⊥] Department of Chemistry, University of Leicester.

[®] Abstract published in *Advance ACS Abstracts*, April 1, 1997.

¹ Abbreviations: CYP 2D6, cytochrome P450 2D6; MPTP, 1-methyl-4-phenyl-1,2,3,6-tetrahydropyridine; PTP, 4-phenyl-1,2,3,6-tetrahydropyridine; p-OH-MPTP, 1-methyl-4-(4'-hydroxyphenyl)-1,2,3,6-tetrahydropyridine; P450 reductase, NADPH–cytochrome P450 reductase.

Chart 1: Structures of MPTP (1-Methyl-4-phenyl-1,2,3,6-tetrahydropyridine), PTP (4-Phenyl-1,2,3,6-tetrahydropyridine), and *p*-OH-MPTP [1-Methyl-4-(4'-hydroxyphenyl)-1,2,3,6-tetrahydropyridine]^a



^a The numbering scheme used for the protons of MPTP is shown.

(endogenous or environmental) was involved in the pathogenesis of this disease, and there is some evidence that supports this idea. First, cases of amyotrophic lateral sclerosis and Parkinsonism—dementia found in three separate populations in the western Pacific region appear to be the result of slow-acting toxins present in the seed of the *Cycas* plant used as a foodstuff (Spencer *et al.*, 1993). Second, 1-methyl-4-phenyl-1,2,3,6-tetrahydropyridine (MPTP; Chart 1), a contaminant of illicit meperidine preparations, causes Parkinsonism symptoms in man that are clinically identical to those of the idiopathic disease (Ballard *et al.*, 1985), and that are accompanied by very similar degeneration of the dopaminergic neurons of the *pars compacta* of the *substantia nigra* (Burns *et al.*, 1983; Langston *et al.*, 1983), providing further evidence that such symptoms can indeed be produced by a neurotoxin. We and others have shown that CYP 2D6 metabolizes and detoxifies MPTP (Coleman *et al.*, 1996; Gilham *et al.*, 1997) and that the enzyme is expressed in the susceptible neurons of the *substantia nigra* (Gilham *et al.*, 1997), providing a possible rationale for the association of defective drug metabolism with increased susceptibility to Parkinson's disease.

We recently reported the expression of CYP 2D6 in baculovirus and its purification in milligram quantities for structural studies (Paine *et al.*, 1996; Modi *et al.*, 1996a). This allowed us to use NMR to determine distances from the heme iron to protons of a bound substrate, codeine, and to combine this data with a multiple sequence and structure alignment of the known crystal structures of P450s to construct a model of the CYP 2D6—codeine complex (Modi *et al.*, 1996a). Codeine binds to the enzyme so that the methoxy group is directly above the A ring of the heme, while the basic nitrogen interacts with the carboxylate of aspartate 301 (Ellis *et al.*, 1995; Modi *et al.*, 1996a). Most 2D6 substrates have a basic nitrogen, and it is likely that an interaction between this and Asp301 is a common feature of many CYP 2D6—substrate complexes. However, MPTP

has been shown to be metabolized by CYP 2D6 by N-demethylation to 4-phenyl-1,2,3,6-tetrahydropyridine (Coleman *et al.*, 1996; Gilham *et al.*, 1997), implying that this substrate binds with its basic nitrogen close to the heme and hence relatively distant from Asp301 (in our models of the CYP 2D6—codeine complex the carboxylate oxygens of Asp301 are 8–11 Å from the heme iron; Modi *et al.*, 1996a).

We now report studies of the interaction of MPTP with cytochrome P450 2D6 and the construction of a model for the enzyme—substrate complex on the basis of NMR-derived distance constraints. We show that the addition of human NADPH—cytochrome P450 reductase leads to a change both in the mode of binding of MPTP to CYP 2D6 and in the products formed, indicating that the interaction between these two enzymes leads to an allosteric change in the active site of CYP 2D6.

MATERIALS AND METHODS

Materials. His-Bind resin was obtained from Novagen; PD10 and Mono Q (5/5) FPLC columns were from Pharmacia. All media were obtained from Gibco. MPTP·HCl was purchased from SEMAT Biochemicals (St. Albans, U.K.). Codeine, buproralol, and thrombin were obtained from Sigma; all other chemicals used were at least analytical grade.

Protein Expression and Purification. Cytochrome P450 2D6 for NMR experiments was expressed in a baculovirus/Sf9 cell system using the vector pMP462 described recently (Paine *et al.*, 1996; Modi *et al.*, 1996a). The cDNA for human NADPH—cytochrome P450 reductase was obtained from a human skin fibroblast cDNA library by PCR (Smith *et al.*, 1994). After amplification and digestion, the cDNA was ligated into the unique *NdeI/XhoI* sites of the *Escherichia coli* expression plasmid pET15b (Novagen), which puts a His₆ linker and a thrombin cleavage site onto the N-terminus of the expressed protein. Both proteins were purified by nickel—agarose affinity chromatography (Arnold, 1991) and the His-tag was removed by thrombin cleavage as previously described (Modi *et al.*, 1996a; Zhao *et al.*, 1996). The concentration of CYP 2D6 was measured by the method of Omura and Sato (1964) using $\epsilon = 91 \text{ mM}^{-1} \text{ cm}^{-1}$ at 448 nm for the reduced CO complex.

Isolation and Identification of MPTP Metabolites. In order to allow sufficient quantities of the products of CYP 2D6 action on MPTP to be isolated, 15 mL reaction mixtures containing 30 μM CYP2D6 and 5 mM MPTP in 0.1 M phosphate buffer, pH 8.0, with either 600 μM cumene hydroperoxide or 60 μM human reductase and an NADPH regenerating system (0.33 mM glucose 6-phosphate, 0.13 mM NADP⁺, 0.33 mM MgCl₂, and 0.4 unit of glucose-6-phosphate dehydrogenase) were incubated in open beakers for 10 h. The reaction was stopped by the addition of 10 mL of 1 M NaOH. The solutions were extracted twice with 10 mL of ethyl acetate, and the combined extracts were evaporated to dryness under nitrogen. The residue was dissolved in 5 mL of HPLC buffer (0.1 M sodium acetate, 0.075 M TEA·HCl, adjusted to pH 2.7 with formic acid, and 10% acetonitrile) and 100 μL was loaded onto an HPLC column (Phase Sep, SCX 250 \times 4.6 mm) and eluted isocratically. The isolated metabolites were identified by NMR and mass spectrometry.

Optical Spectroscopy. UV—visible spectra were obtained at 4 °C as described previously (Modi *et al.*, 1995a,b, 1996a).

Equilibrium constants for substrate binding were estimated by fitting the following equation [see, *e.g.*, He *et al.* (1991)] to the changes in absorbance at 418 nm:

$$\Delta A = \frac{\Delta A_{\infty}}{2E} [E + S + K_d - \{E + S + K_d\}^2 - 4ES]^{1/2} \quad (1)$$

where E and S represent the concentrations of CYP 2D6 and substrate, respectively, ΔA and ΔA_{∞} are the changes in absorption at, respectively, the substrate concentration S and at saturating substrate concentration, and K_d is the equilibrium dissociation constant of the enzyme–substrate complex.

NMR Spectroscopy. Proton NMR measurements were carried out predominantly at 600 MHz, using a Bruker AMX600 spectrometer; studies of the frequency dependence of relaxation rates additionally involved measurements at 300 and 500 MHz. Paramagnetic relaxation experiments were carried out and the data were analyzed as described previously (Modi *et al.*, 1995a, 1996a); the reduced enzyme was prepared as described by Modi *et al.* (1996b). Measurements of T_1 were made at 4 °C by the inversion recovery method, fitting the data by a single exponential. After each set of experiments, optical spectra of the reduced CO complex were measured to ensure that CYP 2D6 had not been converted into inactive P420 during the course of the NMR experiments. For a single mode of substrate binding (one MPTP molecule binding to the active site in a single orientation), the longitudinal relaxation rate, $R_{1,obs}$, is given by [Modi *et al.*, 1995a; see also Lian and Roberts (1993)]:

$$(R_{1,obs} - R_{1,d}) - R_{1,f} = \frac{E_0}{K_d + S_0} (R_{1,P} - R_{1,f}) \quad (2)$$

where E_0 and S_0 are the total enzyme and substrate concentrations, respectively ($S_0 \gg E_0$), and K_d is the dissociation constant of the enzyme–substrate complex. $R_{1,P}$ is the paramagnetic contribution to the relaxation rate of the protons in the bound substrate (due to the unpaired electrons of the heme iron), $R_{1,d}$ is the relaxation rate measured under the same conditions but with a diamagnetic control, in this case the reduced carbon monoxide complex of the enzyme, and $R_{1,f}$ is the relaxation rate of the free substrate. (The MPTP proton relaxation rates in the presence of the reduced CO complex at the same concentrations were found to be identical to those in buffer, indicating that the diamagnetic contribution to relaxation was negligible.) Fitting eq 2 to measurements of $(R_{1,obs} - R_{1,d})$ as a function of protein and/or substrate concentration provides estimates of K_d and $R_{1,P}$; the concentration ranges used were 1–30 μ M enzyme and 1–30 mM MPTP. When the binding of MPTP is measured in the presence of bufuralol, the apparent K_d for MPTP, $K_{d,app}$, is related to the true dissociation constants, $K_{d,MPTP}$ and $K_{d,bufuralol}$, by (Birdsall *et al.*, 1981):

$$K_{d,app} = K_{d,MPTP} + [\text{bufuralol}] \frac{K_{d,MPTP}}{K_{d,bufuralol}} \quad (3)$$

For the case in which only one molecule of MPTP can bind to the active site of the enzyme, but in one of two alternative orientations, A and B, eq 2 is replaced by

$$(R_{1,obs} - R_{1,d}) - R_{1,f} = \frac{E_0 - \frac{E_0}{K_{d,B} + S_0}}{K_{d,A} + S_0} (R_{1P,A} - R_{1,f}) + \frac{E_0 - \frac{E_0}{K_{d,A} + S_0}}{K_{d,B} + S_0} (R_{1P,B} - R_{1,f}) \quad (4)$$

where $R_{1P,A}$, $R_{1P,B}$ and $K_{d,A}$, $K_{d,B}$ are the relaxation rates and dissociation constants of MPTP bound in modes A and B.

The paramagnetic contribution, $R_{1,P}$, to the relaxation rate of the protons of bound substrate arising from the unpaired electrons on the heme iron is related to the iron–proton distance by the Solomon–Bloembergen equation (Solomon & Bloembergen, 1956; Dwek, 1973; Jardetzky & Roberts, 1981):

$$R_{1,P} = \frac{1}{T_{1,M}} = \frac{2}{15} \frac{\gamma_I^2 g^2 S(S+1) \beta^2}{r^6} \left(\frac{3\tau_c}{1 + \omega_I^2 \tau_c^2} + \frac{7\tau_c}{1 + \omega_S^2 \tau_c^2} \right) \quad (5)$$

where r is the distance of the proton from the heme iron, ω_I and ω_S are the nuclear and electronic Larmor frequencies, respectively, and τ_c is the effective correlation time of the dipolar interaction. The assumptions underlying the use of this equation are outlined in Jardetzky and Roberts (1981); see also Modi *et al.* (1995a, 1996a). The correlation time (τ_c) was estimated by measuring $R_{1,P}$ at three frequencies (300, 500, and 600 MHz) and fitting eq 5 to the data; a value of 3×10^{-10} s was obtained.

Modeling of the Complexes of MPTP with CYP 2D6. A set of models of the CYP 2D6–MPTP complex were produced using a combination of homology modeling and distance restraints obtained from the paramagnetic relaxation data. The approach adopted was similar to that used previously for modeling the CYP 2D6–codeine complex (Modi *et al.*, 1996a). In brief, we used a structure-based multiple sequence alignment essentially identical to that in Modi *et al.* (1996a) (differing only by the inclusion of P450 eryF; see supporting information), together with the structures of the four cytochromes P450 available from the Brookhaven Protein Data Bank (PDB; Bernstein *et al.*, 1977; Abola *et al.*, 1987): P450 cam (PDB accession number 2CPP; Poulos *et al.*, 1987), P450 terp (1CPT; Hasemann *et al.*, 1994), P450 BM3 (2HPD; Ravichandran *et al.*, 1993), and P450 eryF (1OXA; Cupp-Vickery & Poulos, 1995). A total of 120 models were produced and refined using the program MODELLER (Sali & Blundell, 1993); these consisted of four sets of models, having either the basic nitrogen or the aromatic ring of MPTP close to the heme iron, both with and without a distance restraint between the basic nitrogen and the carboxylate of Asp 301. These models were built containing only heavy atoms (*i.e.*, no hydrogens), as the four crystal structures on which the models are based do not contain hydrogen atoms, and in any case the resulting models are likely only to be a first approximation to the three-dimensional structure of CYP 2D6. The position of the MPTP was defined partly by nonbonded intermolecular interactions between itself and the protein or the heme, partly by the distance restraints derived from the paramagnetic

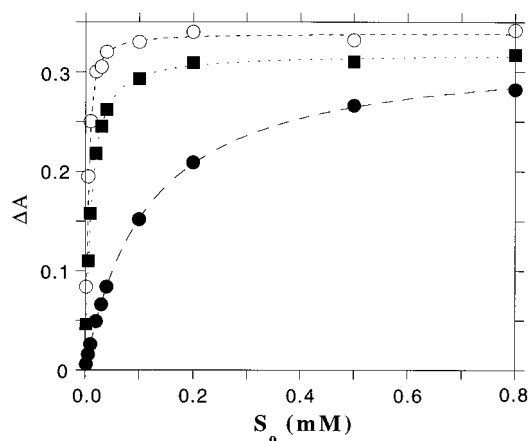


FIGURE 1: Changes in absorbance at 418 nm for CYP 2D6 (5.2 μ M) in 0.1 M phosphate buffer (pH 8.0) at 4 $^{\circ}$ C as a function of the concentration of MPTP (●), codeine (■), and bufuralol (○). The lines are the least-squares fits of eq 1 to the data.

relaxation data, and in two of the four sets of models, partly by the distance restraint (range 2.5–4.5 \AA) between the basic nitrogen of MPTP and OD1 on Asp 301. The conformation of bound MPTP was determined by these interactions and by the bond length, bond angle, torsion angle, and improper angle terms in the CHARMM force field used in MODELLER. A total of 16 experimental restraints, defining 8 upper and 8 lower distance bounds, were used; these were defined in terms of the carbon atom to which the respective proton is bonded. Lower bounds were then defined as the experimentally determined $\text{Fe}\cdots\text{H}$ distance minus 10% (a liberal estimate of the possible error in this measurement) minus 1 \AA (the CH bond length), and upper bounds as the experimentally determined distance plus 10% plus 1 \AA . For the magnetically equivalent aromatic protons (H8 and H10; H7 and H11) an additional correction of 2 \AA was added. Conformational clustering of the final models, and identification of structures “representative” of the ensemble of models, were performed using the program NMRCCLUS (Kelley *et al.*, 1996).

RESULTS AND DISCUSSION

Binding of MPTP and Bufuralol to CYP 2D6. On addition of increasing concentrations of the substrates MPTP or bufuralol to CYP 2D6, changes in the optical absorbance spectrum typical of the “type I” spectral changes seen on substrate binding to cytochromes P450 are observed: the intensity of the Soret band of the oxidized enzyme at 418 nm decreases, while the intensity of bands at 390 and 650 nm increases (data not shown). The dependence of these optical changes on substrate concentration (Figure 1) can be used to estimate the equilibrium constant for substrate binding; the values obtained for MPTP, codeine, and bufuralol are summarized in Table 1. The magnitude of the change in absorbance is in each case consistent with a complete spin-state conversion at saturating substrate concentrations. The equilibrium constant for MPTP binding can also be determined from the concentration dependence of the paramagnetic relaxation effects of the heme iron on the MPTP protons, provided that exchange of the substrate between the free and bound states is sufficiently rapid. The spin–lattice relaxation rate ($R_{1,\text{obs}}$) of MPTP protons in the presence of the enzyme was measured in 0.1 M phosphate buffer, pH 8.0, over the range 277–293 K; a linear increase

Table 1: Substrate Binding to Recombinant CYP 2D6

substrate	method ^a	K_d (μ M)
MPTP	optical	110 (\pm 12)
	NMR	149 (\pm 22)
	NMR competition	129 (\pm 38)
bufuralol	optical	2.2 (\pm 0.3)
	NMR competition	2.4 (\pm 0.4)
codeine	optical	7.4 (\pm 0.7)

^a Optical: from absorbance changes at 418 nm, at 5–10 μ M enzyme (eq 1). NMR: from paramagnetic relaxation effects on MPTP protons, at 30 μ M enzyme (eq 2). NMR competition: values calculated using eq 3 from NMR-determined apparent K_d values for MPTP at various concentrations of bufuralol. All experiments were carried out at 4 $^{\circ}$ C in 0.1 M phosphate buffer, pH 8.0.

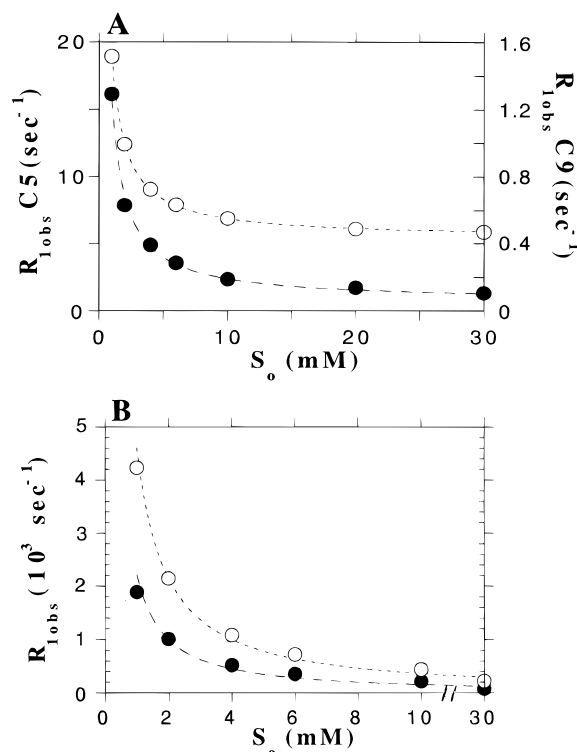


FIGURE 2: Measured spin–lattice relaxation rates for protons of MPTP as a function of MPTP concentration in the presence of CYP 2D6 in 0.1 M phosphate buffer, pH 8.0, at 4 $^{\circ}$ C. (A) With 30 μ M CYP 2D6: (●) C5H, (○) C9H. Lines represent the least-squares fit of eq 2 to the experimental data. (B) With 30 μ M CYP 2D6 and 100 μ M P450 reductase: (●) $-\text{NCH}_3$, (○) C9H. Lines represent the least-squares fit of eq 2 to the experimental data, yielding K_d = 149 μ M for $-\text{NCH}_3$ and K_d = 25 μ M for C9H.

in $R_{1,\text{obs}}$ as a function of reciprocal temperature was observed, demonstrating that the fast exchange condition is satisfied in this case (data not shown). The average K_d value determined from measurements on all the protons of MPTP (Figure 2) is 149 μ M, in reasonable agreement with the value obtained from optical spectroscopy. As can be seen from Table 1, MPTP binds weakly compared to bufuralol or codeine. Further confirmation that MPTP does bind in the active site was obtained by carrying out competition experiments between MPTP and the well-known CYP 2D6 substrate bufuralol, using spin–lattice relaxation measurements. The dependence of the relaxation rate of MPTP protons on MPTP concentration was measured at each of seven bufuralol concentrations, and eq 2 was fitted to the data for each MPTP resonance to obtain values of the apparent dissociation constant, $K_{d,\text{app}}$, for MPTP at each

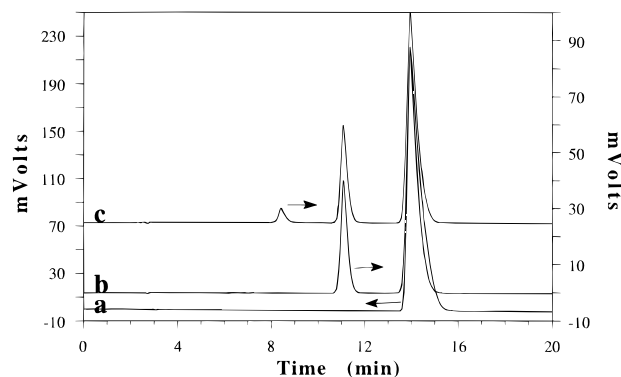


FIGURE 3: HPLC profiles of (a) MPTP, (b) an extract of a reaction mixture containing MPTP, CYP 2D6, and cumene hydroperoxide, and (c) an extract of a reaction mixture containing MPTP, CYP 2D6, P450 reductase, and an NADPH-regenerating system. The arrows indicate the relevant scales; trace c has been offset vertically by 25 mV for clarity.

bufuralol concentration (see supporting information). These $K_{d,app}$ values were found to increase linearly with the bufuralol concentration, as predicted by eq 3, and the K_d values for MPTP and bufuralol binding obtained from the analysis of the data in terms of eq 3 agreed well with the values obtained for the two ligands separately by optical and NMR methods (Table 1). This demonstrates that MPTP and bufuralol compete with each other for binding to the same site on CYP 2D6.

The changes in the absorbance spectrum on substrate binding have been attributed to a change in spin state of the heme iron from low spin ($S = 1/2$) to high spin ($S = 5/2$) (Dawson, 1988; Sariaslani, 1991). The crystal structures of cytochromes P450 show that in the absence of substrate a water molecule (or a hydroxide ion) is present in the sixth coordination position of the heme iron (e.g., Poulos *et al.*, 1987; Ravichandran *et al.*, 1993), and this is expelled on binding of the substrate (e.g., Poulos *et al.*, 1987; Modi *et al.*, 1995a). The presence of a strong-field (aquo) ligand axially coordinated to the iron atom leads to maximal pairing

of the 5 d electrons of the iron to give a net spin of $1/2$, whereas on substrate binding the absence of such a strong-field ligand leads to maximal unpairing of the d electrons to give a net spin of $5/2$. These changes in the optical spectrum are thus consistent with MPTP binding to CYP 2D6 in a manner involving displacement of the coordinated water molecule and hence typical of a substrate.

Identification of the Products Formed by the Action of CYP 2D6 on MPTP. As reported earlier (Gilham *et al.*, 1997), when MPTP is incubated with recombinant CYP 2D6 in the presence of cumene hydroperoxide as oxygen and electron donor, a single metabolite is observed on HPLC separation of the ethyl acetate extract of the reaction mixture (Figure 3). However, when the incubation was carried out with NADPH-cytochrome P450 reductase and an NADPH-regenerating system in place of cumene hydroperoxide, an additional metabolite was observed (Figure 3).

The metabolite observed in both incubations has been identified by mass spectrometry (mass 159, *vs* 173 for MPTP) and NMR (Figure 4) as 4-phenyl-1,2,3,6-tetrahydropyridine (Chart 1, PTP; Gilham *et al.*, 1997). In the NMR spectrum of PTP, the pairs of methylene protons on carbons 2, 3, and 6 are more nearly magnetically equivalent than in MPTP. This can be explained by more rapid nitrogen inversion and/or ring inversion in PTP than in MPTP; similar shift differences are seen on comparing piperidine and *N*-methylpiperidine (Booth, 1969). The additional metabolite formed when P450 reductase is used as the source of electrons has a molecular mass of 189 (compared to 173 for MPTP), suggesting that it is a hydroxylated metabolite of MPTP; the NMR spectrum of this compound (Figure 4) shows that it has an electronegative substituent at the *para* position of the phenyl ring, while the resonances of the tetrahydropyridine ring protons appear at the same positions as in MPTP. This second metabolite is thus identified as 1-methyl-4-(4'-hydroxyphenyl)-1,2,3,6-tetrahydropyridine (pOH-MPTP; Chart 1).

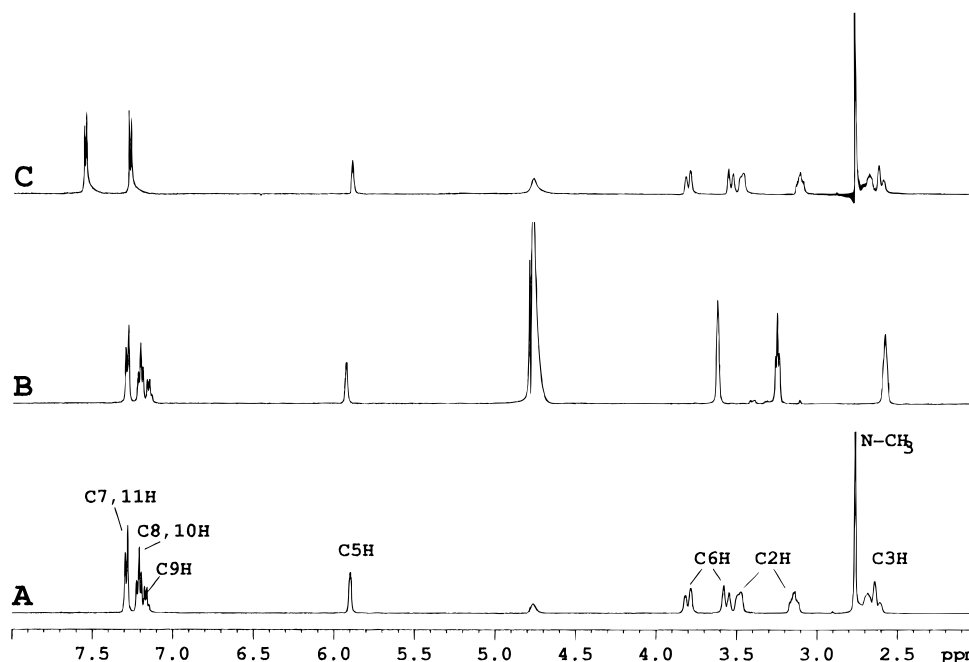


FIGURE 4: Proton NMR spectra (600 MHz) of MPTP (A) and its two metabolites PTP (B) and pOH-MPTP (C) in 0.1 M phosphate buffer, pH 8.0, at 277 K.

Table 2: Paramagnetic Relaxation Times and Distances from the Protons of Bound MPTP to the Heme Iron of CYP 2D6

proton ^a	$T_{1,M}$ (ms)	r (Å)
-NCH ₃	0.014 (\pm 0.002)	3.4 (\pm 0.2)
C2H ^A	0.069 (\pm 0.004)	4.4 (\pm 0.1)
C2H ^B	0.35 (\pm 0.03)	5.8 (\pm 0.1)
C3H ^A	0.47 (\pm 0.04)	6.1 (\pm 0.1)
C3H ^B	1.2 (\pm 0.1)	7.1 (\pm 0.2)
C5H	1.8 (\pm 0.2)	7.7 (\pm 0.3)
C6H ^A	0.21 (\pm 0.02)	5.4 (\pm 0.1)
C6H ^B	0.70 (\pm 0.05)	6.5 (\pm 0.2)
C7H, C11H	3.9 (\pm 0.3)	8.7 (\pm 0.2)
C8H, C10H	15.5 (\pm 1.0)	11.0 (\pm 0.3)
C9H	24.8 (\pm 1.2)	11.9 (\pm 0.3)

^a See Chart 1 for proton nomenclature; the individual protons of the methylene groups at positions 2, 3, and 6, indicated as A and B, have not been stereospecifically assigned.

The K_m value for the formation of PTP was found to be 134 μ M in reactions supported by cumene hydroperoxide and 120 μ M with P450 reductase as electron donor; these values are similar to one another and to the K_d values for MPTP binding to CYP 2D6 alone determined by optical and NMR spectroscopy (Table 1). The K_m value for the formation of pOH-MPTP was measured as 19 μ M. This clearly suggests that in the presence of P450 reductase MPTP must form two different complexes with CYP 2D6, which have different affinities and lead to different products.

Structural Studies of MPTP Binding. In order to obtain direct evidence for possible alternative modes of MPTP binding to CYP 2D6, we have used measurements of the paramagnetic relaxation effects of the heme iron on the protons of the MPTP to obtain estimates of distances between individual protons of the bound substrate and the heme iron, as described previously for P450 BM3 and 2D6 (Modi *et al.*, 1995a, 1996a,b). The paramagnetic contribution to the proton spin–lattice relaxation rates of the bound substrate were determined by fitting eq 2 to data of the kind shown in Figure 2. Experiments were carried out at two different protein concentrations (1 and 30 μ M) to permit precise measurements for all the resolved proton resonances.

The spin–lattice relaxation times of the bound substrate, $T_{1,M}$, and the estimated iron–proton distances for MPTP bound to CYP 2D6 in the absence of the reductase are summarized in Table 2. These measurements give a very clear indication of the orientation of the MPTP molecule in the active site of the enzyme, the protons of the N-methyl group being only 3.4 Å away from the heme iron, while the ring protons of phenyl group are 9–12 Å away. This is clearly in accord with the observation that CYP 2D6, with cumene hydroperoxide as oxygen and electron donor, catalyzes N-demethylation of MPTP. As noted above, for MPTP binding to CYP 2D6 alone, the K_d estimated from the NMR data is in satisfactory agreement with that obtained from optical spectroscopy (Table 1); fitting the NMR data with a version of eq 2 in which the stoichiometry is a variable gave an estimate of 1.0 (\pm 0.2) molecules of MPTP bound per molecule of CYP 2D6. Thus under these conditions there appears to be a single mode of binding of MPTP molecule, in a position and orientation which correctly predicts the formation of an N-demethylated product. We have recently shown that, in the case of cytochrome P450 BM3 from *Bacillus megaterium*, there is a substantial movement of the bound substrate on reduction of the enzyme (Modi *et al.*,

1996b); no such effect was detected with MPTP binding to CYP 2D6, and relaxation experiments with the ferrous state of the enzyme gave iron–proton distances indistinguishable from those obtained with the ferric state (data not shown).

Corresponding relaxation experiments were carried out in the presence of NADPH–cytochrome P450 reductase, in a 2-fold excess over CYP 2D6, and the results are given in Figure 2B and Table 3. Two features of these results cannot be reconciled with a single mode of binding of MPTP under these conditions. First, while in the absence of the reductase the K_d values obtained from the relaxation data on each proton are in good agreement (Figure 2A), this is not the case in the presence of the reductase (Figure 2B). Estimates of K_d vary from 140 μ M for -NCH₃ to 25 μ M for C9H of MPTP. Second, the iron–proton distances estimated on the basis of a single mode of binding were found to be closely similar for the two ends of the molecule [*i.e.*, $d(\text{Fe}\cdots\text{NCH}_3) = 3.4$ Å, $d(\text{Fe}\cdots\text{C9H}) = 3.0$ Å], while protons in the middle of the molecule are 7–9 Å from the iron (Table 3). Given the covalent geometry of MPTP, these distances cannot be accommodated by a single mode of binding. They can, however, be explained on the basis of two alternative modes of binding, by recalling that $1/T_{1,M} \propto 1/r^6$ (eq 5), so that for a given proton, the mode of binding in which this proton is closer to the iron will have a dominant effect on the relaxation. For example, if the -NCH₃ group is close to the iron in one mode of binding (denoted A) but more than twice as far away in the other (B), the observed relaxation effects will be dominated by mode A, and both the iron–proton distance and the K_d will reflect essentially only binding in mode A. If, by contrast, C9H is close to the iron in mode B and distant in mode A, its relaxation behavior will be dominated by binding in mode B and will give a distance and a K_d value apparently inconsistent with the values obtained from the -NCH₃ resonance. The data were quantitatively analyzed in terms of a “two binding mode model” by fitting the concentration dependence of relaxation for all the resonances with eq 4, which corresponds to a model in which only a single MPTP molecule can bind to the enzyme, but in two alternative orientations. This equation was able to fit the data for all the protons of MPTP with two values of K_d , 149 (\pm 22) μ M for mode A (in which the N-methyl group is close to the iron), and 25 (\pm 3) μ M for mode B (in which C9H is close to the iron), and gave distances which were consistent with the structure of MPTP.

The $T_{1,M}$ values and the derived distances obtained from this analysis are given in Table 3. The mode of binding denoted A is clearly essentially identical to that observed in the absence of reductase, in terms of the position and orientation of the substrate. The K_d for mode A binding is very similar to that calculated in the absence of reductase and also to the K_M value associated with the formation of PTP, whether in the presence or absence of reductase. In mode B, however, MPTP binds almost 10-fold more tightly, and in a very different orientation, with the *para* position of the aromatic ring closest to the iron. This orientation corresponds to that expected for the formation of the second product, pOH-MPTP, which is hydroxylated in the *para* position of the aromatic ring, and indeed the K_d estimated for this mode of binding is close to the K_M value for formation of this product.

Structural Models of the CYP 2D6–MPTP Complexes. Models for the two modes of binding of MPTP to CYP 2D6

Table 3: Paramagnetic Relaxation Times and Distances from the Protons of the Bound MPTP to the Heme Iron of CYP 2D6 in the Presence of Human P450 Reductase

proton	two alternative modes of binding ^b					
	single binding mode ^a		A		B	
	$T_{1,M}$ (ms)	r (Å)	$T_{1,M}$ (ms)	r (Å)	$T_{1,M}$ (ms)	r (Å)
–NCH ₃	0.014 (± 0.002)	3.4 (± 0.2)	0.013 (± 0.002)	3.4 (± 0.2)	31.5 (± 2)	12.4 (± 0.6)
C2H ^A	0.069 (± 0.004)	4.5 (± 0.1)	0.068 (± 0.004)	4.4 (± 0.1)	16.2 (± 1)	11.1 (± 0.5)
C2H ^B	0.36 (± 0.03)	5.9 (± 0.1)	0.34 (± 0.04)	5.8 (± 0.1)	14.5 (± 1.2)	10.9 (± 0.7)
C3H ^A	0.52 (± 0.03)	6.2 (± 0.1)	0.47 (± 0.04)	6.1 (± 0.1)	4.9 (± 0.2)	9.1 (± 0.4)
C3H ^B	1.6 (± 0.1)	7.5 (± 0.2)	1.2 (± 0.2)	7.1 (± 0.2)	4.4 (± 0.2)	8.9 (± 0.2)
C5H	4.6 (± 0.2)	9.0 (± 0.2)	1.9 (± 0.3)	7.7 (± 0.3)	2.9 (± 0.2)	8.3 (± 0.6)
C6H ^A	0.22 (± 0.02)	5.4 (± 0.1)	0.21 (± 0.02)	5.4 (± 0.1)	12.0 (± 0.8)	10.5 (± 0.5)
C6H ^B	0.74 (± 0.06)	6.6 (± 0.2)	0.71 (± 0.02)	6.6 (± 0.1)	12.7 (± 0.9)	10.6 (± 0.5)
C7H, C11H	1.19 (± 0.09)	7.2 (± 0.2)	3.9 (± 0.4)	8.7 (± 0.2)	0.92 (± 0.08)	6.9 (± 0.4)
C8H, C10H	0.08 (± 0.005)	4.5 (± 0.1)	14.8 (± 1.5)	10.9 (± 0.4)	0.075 (± 0.007)	4.5 (± 0.2)
C9H	0.0069 (± 0.0006)	3.0 (± 0.1)	25 (± 2)	11.9 (± 0.4)	0.0069 (± 0.0005)	3.0 (± 0.1)

^a From fitting data with eq 2. ^b From fitting data with eq 4.

in the presence of P450 reductase were constructed by a combination of homology modeling and the use of constraints derived from the relaxation data [see Materials and Methods and Modi *et al.* (1996a)]. As can be seen from Tables 2 and 3, the estimated distances for MPTP binding in mode A are essentially identical in the presence and absence of the reductase, and a single set of models was generated for this mode of binding. A total of 120 models of the CYP 2D6–MPTP complex were generated: 40 with the basic nitrogen close to the heme iron (mode A), 20 of which included a restraint for a possible interaction between Asp 301 and the basic nitrogen (as observed for codeine; Ellis *et al.*, 1995; Modi *et al.*, 1996), and 80 with the aromatic ring close to the heme iron (mode B), 40 of which included a restraint for a possible interaction between Asp 301 and the basic nitrogen (henceforth abbreviated “Asp–N restraint”). These models were evaluated on the basis of their bonded and nonbonded interactions and their agreement with the NMR-derived distance restraints (and the Asp–N restraint where applicable).² The MPTP binding site (defined as side-chain atoms closer than 5.0 Å to the MPTP in the majority of models) is predominantly hydrophobic in nature in all models. MPTP lies across the A ring of the heme. In the majority of the models, the N-methyl group of MPTP was in an equatorial orientation, as observed in the crystal structure of free MPTP (Klein *et al.*, 1985). It is important to emphasize that since the effect of the reductase on MPTP binding most likely arises from changes in the conformation of the active site (see below), the models shown in Figure 5, particularly that of binding mode B, can at this stage only be very approximate.

Of the 40 models generated for binding mode A (with the N-methyl of MPTP close to the heme), 25 were discarded, leaving 15 models (9 with and 6 without the Asp–N restraint) that were taken as acceptable representations of the three-dimensional structure of the complex (Figure 5a,b). Clustering the orientations of MPTP in these models does not distinguish between models with and those without the Asp–N restraint, although this restraint does increase the probability of the N-methyl group of MPTP adopting an axial orientation. Thus, it appears that introduction of a restraint corresponding to an interaction between the basic nitrogen

of MPTP and the carboxylate of Asp301 does not affect the positioning of MPTP in the binding site in binding mode A. This is supported by the observation that the Asp301 → Asn mutant of CYP 2D6 catalyzes the N-demethylation of MPTP (with cumene hydroperoxide as oxygen and electron donor) at the same rate as does the wild-type enzyme (G. Smith, personal communication). The lack of this interaction presumably contributes to the weaker binding of MPTP as compared to bufuralol and codeine; in the case of codeine, NMR data shows that the basic nitrogen is close to Asp301 (Modi *et al.*, 1996a).

In binding mode A, the MPTP binding site comprises residues Pro 102 (in 10 out of 15 models), Pro 103 (11/15), Ile 106 (9/15), Thr 107 (9/15), Leu 110 (11/15), and Leu 121 (12/15) in “substrate recognition site 1” (SRS-1; Gotoh, 1992); Asp 301 (13/15), Ala 305 (15/15), and Thr 309 (11/15) in SRS-4; Val 370 (8/15) in SRS-5; and Phe 481 (9/15) and Phe 483 (13/15) in SRS-6. In the “most representative” model [as defined by Kelley *et al.* (1996)], the N-methyl carbon of MPTP is positioned 4.7 Å away from the heme iron (range 2.8–4.8 Å across the set of 15 models), and the N–CH₃ bond is oriented such that it could react with an oxygen bound to the heme iron (Figure 5a,b).

For binding mode B, with C9H close to the heme iron, 17 acceptable models were obtained, 9 with and 8 without the Asp–N restraint. Clustering the orientations of MPTP in models from these two sets places the models into three clusters, one cluster containing all those models generated with the Asp–N restraint plus one determined without (10 models in total); the other two clusters contain models obtained without this restraint (4 models in one cluster, 3 in the other). Thus, in binding mode B, the introduction of the Asp–N restraint does affect the positioning of MPTP in the binding site. In the absence of the Asp–N restraint, the MPTP binding site consists of residues Leu 110 (in 6 out of 8 models), Leu 121 (6/8), Ser 304 (5/8), Ala 305 (8/8), Thr 309 (7/8), Val 370 (5/8), Phe 483 (8/8), and Leu 484 (5/8); the side chain of Asp 301 is within 5 Å of MPTP in 3 out of 8 models. In the most representative model, the nitrogen of MPTP is 10.7 Å from the heme iron (range 9.4–10.7 Å across the set of 8 models). The C9 carbon of the aromatic ring is 4.3 Å from the heme iron (range 3.1–4.3 Å), and the C9–H9 bond is oriented such that it could possibly react with an oxygen bound to the heme iron (Figure 5c,d).

² Confidence in residues 1–27 of the models is low, because of the absence of structural information for these residues. Coordinates of the final models are available on email request to gcr@le.ac.uk.

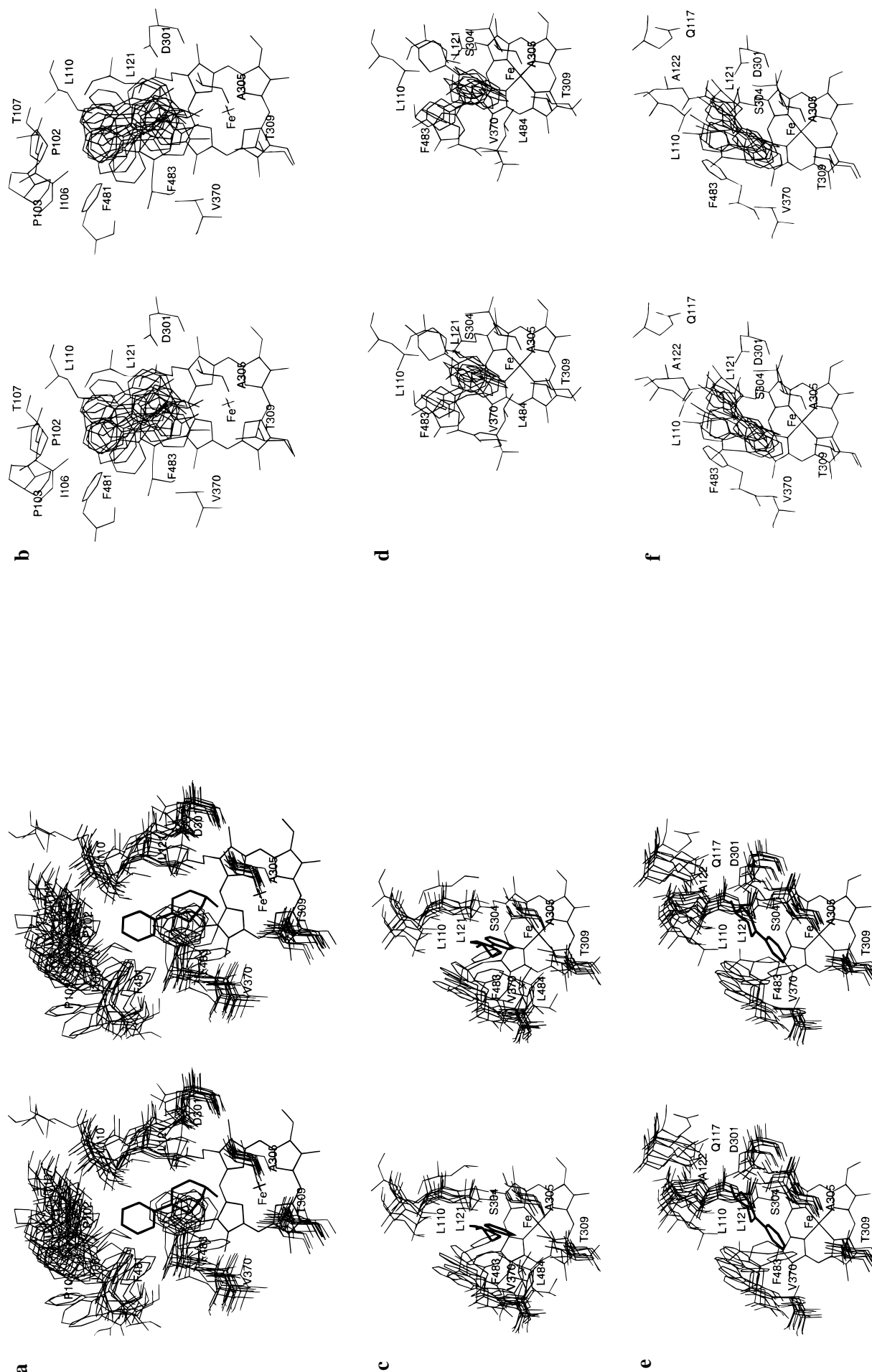


FIGURE 5: Stereoviews of models of MPTP in its binding site on CYP 2D6 following superposition of the heme moieties. (a, b) The 15 final models determined in binding mode A. (c, d) The 8 final models determined in binding mode B, with no Asp-N restraint. (e, f) The 9 final models determined in binding mode B, with the Asp-N restraint included. In (a, c, e), a single MPTP molecule (chosen as the "most representative" MPTP orientation using the program NMIRCLUST; Kelley et al., 1996) is shown, with the residues lining the MPTP binding site in all the models. In (b, d, f) the MPTP molecules in all the models are shown, with the residues lining the MPTP binding site in the "most representative" protein in each case.

In the presence of the Asp–N restraint, the MPTP binding site comprises residues Leu 110 (in 9 out of 9 models), Gln 117 (5/9), Leu 121 (9/9), Ala 122 (6/9), Asp 301 (9/9), Ser 304 (8/9), Ala 305 (9/9), Thr 309 (8/9), Val 370 (7/9), and Phe 483 (9/9). The difference in orientation induced by the inclusion of the Asp–N restraint is reflected in the fact that, of these residues, Gln117 and Ala122, as well as Asp301, do not appear in the contact list in the absence of this restraint. However, in spite of this difference, the position of the C9 carbon of the aromatic ring is very similar: 4.2 Å from the heme iron in the most representative orientation (range 3.9–4.4 Å across the set of 9 models), with the C9–H9 bond oriented such that it could possibly react with an oxygen bound to the heme iron (Figure 5e,f). In both sets of models for binding mode B (with and without the Asp–N restraint), the C9–H9 bond could be positioned closer to the iron–oxo species if the I-helix were to move laterally, away from the center of the heme.

Comparison with Codeine Binding. Codeine binds to CYP 2D6 in an orientation in which its methoxy group is closest to the heme iron and its basic nitrogen is close to Asp301, consistent with the observation that, with cumene hydroperoxide as oxygen and electron donor, CYP 2D6 metabolizes codeine by O-demethylation to morphine (Modi *et al.*, 1996a). The binding site defined by using the codeine data is able to accommodate MPTP without adjusting any atoms of the protein. In comparison with the volume occupied in the active site by codeine, in binding mode A the aromatic ring of MPTP tends to lie further away from the I-helix and nearer to Pro 102, while in mode B MPTP occupies a similar volume to codeine when the Asp301–N restraint is present but not when it is absent. We have now studied the metabolism of codeine by CYP 2D6 using NADPH–cytochrome P450 reductase as the source of electrons and have carried out relaxation measurements in the presence of the reductase. In both cases, the presence of the reductase had no effect on the results. A single metabolite, morphine, was still observed, the binding was not significantly affected [$K_d = 93 (\pm 14) \mu\text{M}$ in the presence of reductase, compared to $115 (\pm 23) \mu\text{M}$ in its absence], and the iron–proton distances differed by less than 3% from those reported earlier in the absence of the reductase (Modi *et al.*, 1996a). It appears that the effect of P450 reductase on substrate binding and catalysis by CYP 2D6 is dependent on the particular substrate employed.

Conclusions: Effects of Cytochrome P450 Reductase on CYP 2D6. The observation that the use of NADPH–cytochrome P450 reductase, as opposed to cumene hydroperoxide, to support the action of CYP 2D6 on MPTP leads to the formation of an additional product could have either a chemical or a conformational explanation. Although alkyl hydroperoxides, such as the cumene hydroperoxide used here, undergo heterolysis to produce an oxidizing species similar if not identical to that generated with NADPH and cytochrome P450 reductase, there are potentially significant differences between the two means of supporting the P450-mediated oxygenation reaction. First, the hydroperoxides also undergo homolytic fission to form alkoxy radicals, and second, the alkyl group can remain in the active site long enough to be hydroxylated and/or to alter the action of the enzyme on other substrates (Ortiz de Montellano, 1995). The latter effect might account for a difference in the products formed by the action of CYP 2D6 in the presence of cumene

hydroperoxide as compared to NADPH and P450 reductase. Alternatively, the interaction of P450 reductase with CYP 2D6 might alter the structure of the active site sufficiently to permit an alternative mode of substrate binding.

The NMR experiments allow us to compare the binding of MPTP to CYP 2D6 in the presence and absence of P450 reductase under conditions where no reaction is occurring, and specifically in the absence of cumene hydroperoxide and its possible secondary effects. The finding from these equilibrium experiments that the reductase does indeed alter the binding of MPTP to CYP 2D6, in terms both of affinity and of orientation, shows clearly that a conformational rather than a chemical mechanism must underlie this effect—in other words, the binding of P450 reductase is having an allosteric effect on substrate binding to CYP 2D6.

There have been a number of reports of differential effects of alkyl hydroperoxides, P450 reductase, and/or cytochrome *b*₅ on substrate binding and catalysis by other cytochromes P450 (*e.g.*, Mayuzumi *et al.*, 1993; Hiroya *et al.*, 1994; Yamazaki *et al.*, 1995; Gruenke *et al.*, 1995). For example, in the case of CYP 3A4 the 6 β -hydroxylation of testosterone is dependent on cytochrome *b*₅ (as well as P450 reductase), while the N-demethylation of ethylmorphine is not (Yamazaki *et al.*, 1995). In CYP 1A2, mutagenesis experiments have shown that Glu318, Lys453, and Arg455 are important for the metabolism of 7-ethoxycoumarin supported by P450 reductase but not for that supported by *t*-butyl hydroperoxide (Mayazumi *et al.*, 1993; Hiroya *et al.*, 1995). [In CYP 2D6, the residue corresponding to Glu318 in CYP 1A2 is Val308, in a region of helix I (SRS-4) containing several residues that contact the bound substrate.] It is possible that allosteric effects of redox partner proteins are responsible for some of these observations.

An understanding of the mechanism by which the allosteric effect of the reductase is produced must await a more detailed description of the interaction between the two proteins. A good deal of evidence shows that the reductase binds to the proximal side of P450, on the opposite side of the heme from the substrate binding site, and a direct effect on substrate binding is thus unlikely. A candidate for the reductase binding site is a patch of positive charge seen on the proximal face of the protein in P450 cam and P450 terp, and to a lesser extent in P450 BM3 [see Hasemann *et al.* (1995)]. Among the residues contributing to this positive patch in the bacterial P450s are one or two in helix C, which packs against the N-terminal end of helix I. In the models there are several residues in helix I and in the loop between helices B' and C that contact the bound MPTP and that appear to determine the position of the aromatic ring with respect to the heme in binding mode B (particularly in the presence of the Asp–N restraint). Leu121, in the loop immediately preceding the C-helix, is particularly notable in this connection. One may speculate that reductase binding could result in a change in the position of the C-helix, which in turn results in slight movements of the I-helix and of the B'–C loop containing Leu121, thereby allowing MPTP to bind in the orientation seen in mode B. The effect is seen with MPTP but not with the larger substrate codeine. In our approximate models for the complexes the binding sites for MPTP overlap substantially with that for codeine (see above); either the effects of the reductase are limited to the region in contact with MPTP but not codeine or, perhaps more probably, the size and rigidity of codeine may mean that

only one mode of binding is open to it, irrespective of the presence of the reductase.

ACKNOWLEDGMENT

We are grateful to Andrej Sali for his gift of the program MODELLER and to Jimmy Boyle for technical assistance.

SUPPORTING INFORMATION AVAILABLE

Two figures, showing the sequence alignment used for the modeling and the effects of bufuralol on the binding of MPTP (3 pages). Ordering information is given on any current masthead page.

REFERENCES

- Abola, E. E., Bernstein, F. C., Bryant, S. H., Koetzle, T. F., & Weng, J. (1987) in *Crystallographic databases—information content, software systems, scientific applications* (Allen, F. H., Bergerhoff, G., & Sievers, R., Eds.) pp 107–132, Data Commission of the International Union of Crystallography, Bonn, Germany, and Cambridge and Chester, U.K.
- Arnold, F. H. (1991) *Bio/Technology* 9, 151–156.
- Ballard, P. A., Tetrud, J. W., & Langston, J. W. (1985) *Neurology* 35, 949–956.
- Bernstein, F. C., Koetzle, T. F., Williams, G. J. B., Meyer, E. F., Brice, M. D., Rodgers, J. R., Kennard, O., Shimanovich, T., & Tasumi, M. (1977) *J. Mol. Biol.* 112, 535–542.
- Bertilsson, L. (1995) *Clin. Pharmacokinet.* 29, 192–209.
- Birdsall, B., Hyde, E. I., Burgen, A. S. V., Roberts, G. C. K., & Feeney, J. (1981) *Biochemistry* 20, 7186–7195.
- Booth, H. (1969) *Prog. NMR Spectrosc.* 5, 149–381.
- Coleman, T., Ellis, S. W., Martin, I. J., Lennard, M. S., & Tucker, G. T. (1996) *J. Pharmacol. Exp. Ther.* 277, 685–690.
- Cupp-Vickery, J. R., & Poulos, T. L. (1995) *Nature Struct. Biol.* 2, 144–153.
- Dawson, J. H. (1988) *Science* 248, 433–439.
- Dwek, R. A. (1973) *NMR in Biochemistry*, pp 11–142, Oxford University Press, London.
- Eichelbaum, M., & Gross, A. S. (1990) *Pharmacol. Ther.* 46, 377–394.
- Ellis, S. W., Hayhurst, G. P., Smith, G., Lightfoot, T., Wong, M. M. S., Simula, A. P., Ackland, M. J., Sternberg, M. J. E., Lennard, M. S., Tucker, G. T., & Wolf, C. R. (1995) *J. Biol. Chem.* 270, 29055–29058.
- Gilham, D. E., Cairns, W., Paine, M. J., Modi, S., Roberts, G. C. K., & Wolf, C. R. (1997) *Xenobiotica* 27, 111–125.
- Gough, A. C., Miles, J. S., Moss, J. E., Gaedigk, A., Eichelbaum, M., & Wolf, C. R. (1990) *Nature* 347, 773–776.
- Gotoh, O. (1992) *J. Biol. Chem.* 267, 83–90.
- Gruenke, L. D., Konopka, K., Cadieu, M., & Waskell, L. (1995) *J. Biol. Chem.* 270, 24707–24718.
- Hasemann, C. A., Ravichandran, K. G., Peterson, J. A., & Deisenhofer, J. (1994) *J. Mol. Biol.* 236, 1169–1185.
- Hasemann, C. A., Kurumbail, R. G., Boddupalli, S. S., Peterson, J. A., & Deisenhofer, J. (1995) *Structure* 3, 41–62.
- He, S., Modi, S., Bendall, D. S., & Gray, J. C. (1991) *EMBO J.* 10, 4011–4016.
- Hiroya, K., Murakami, Y., Shimizu, T., Hatano, M., & Ortiz de Montellano, P. R. (1994) *Arch. Biochem. Biophys.* 310, 397–401.
- Jardetzky, O., & Roberts, G. C. K. (1981) *NMR in Molecular Biology*, Chapter 3, Academic Press, New York.
- Kelley, L. A., Gardner, S. P., & Sutcliffe, M. J. (1996) *Protein Eng.* (in press).
- Klein, C. L., Borne, R. F., & Stevens, E. D. (1985) *Pharm. Res.* 192–194.
- Kroemer, H. K., & Eichelbaum, M. (1995) *Life Sci.* 56, 2285–2298.
- Lennard, M. S. (1990) *Pharmacol. Toxicol.* 67, 273–283.
- Lian, L.-Y., & Roberts, G. C. K. (1993) in *NMR of Biological Macromolecules* (Roberts, G. C. K., Ed.) pp 153–182, IRL Press at Oxford University Press, Oxford, U.K.
- Mayuzumi, H., Sambongi, C., Hiroya, K., Shimizu, T., Tateishi, T., & Hatano, M. (1993) *Jpn. J. Biochem.* 32, 5622–5628.
- Meyer, U. A., Skoda, R. C., & Zanger, U. M. (1990) *Pharmacol. Ther.* 46, 297–311.
- Modi, S., Primrose, W. U., Boyle, J., Gibson, C. F., Lian, L.-Y., & Roberts, G. C. K. (1995a) *Biochemistry* 34, 8982–8988.
- Modi, S., Primrose, W. U., Lian, L.-Y., & Roberts, G. C. K. (1995b) *Biochem. J.* 310, 939–943.
- Modi, S., Paine, M. J., Sutcliffe, M. J., Lian, L.-Y., Primrose, W. U., Wolf, C. R., & Roberts, G. C. K. (1996a) *Biochemistry* 35, 4540–4550.
- Modi, S., Sutcliffe, M. J., Primrose, W. U., Lian, L.-Y., & Roberts, G. C. K. (1996b) *Nature Struct. Biol.* 3, 414–417.
- Omura, T., & Sato, R. (1964) *J. Biol. Chem.* 239, 2379–2387.
- Ortiz de Montellano, P. R. (1995) in *Cytochrome P450: Structure, Mechanism and Biochemistry* (Ortiz de Montellano, P. R., Ed.) 2nd ed., pp 245–303, Plenum Press, New York.
- Paine, M. J. I., Gilham, D., Roberts, G. C. K., & Wolf, C. R. (1996) *Arch. Biochem. Biophys.* 328, 143–150.
- Poulos, T. L., Finzel, B. C., & Howard, A. J. (1987) *J. Mol. Biol.* 195, 687–700.
- Price-Evans, D. A., Mahgoub, A., Sloan, T. P., Idle, J. R., & Smith, R. L. (1980) *J. Med. Genet.* 17, 102–105.
- Ravichandran, K. G., Boddupalli, S. S., Hasemann, C. A., Peterson, J. A., & Deisenhofer, J. (1993) *Science* 261, 731–735.
- Sali, A., & Blundell, T. L. (1993) *J. Mol. Biol.* 234, 779–815.
- Sariaslani, F. S. (1991) *Adv. Appl. Microbiol.* 36, 133–178.
- Smith, C. A. D., Gough, A. C., Leigh, P. N., Summers, B. A., Harding, A. E., Maranganore, D. M., Sturman, S. G., Schapira, A. H. V., Williams, A. C., Spurr, N. K., & Wolf, C. R. (1992) *Lancet* 339, 1375–1377.
- Smith, G. C. M., Tew, D. G., & Wolf, C. R. (1994) *Proc. Natl. Acad. Sci. U.S.A.* 91, 8710–8714.
- Solomon, I., & Bloembergen, N. (1956) *J. Chem. Phys.* 25, 261.
- Spencer, P. S., Ludolph, A. C., & Kisby, G. E. (1993) *Envir. Res.* 62, 106–113.
- Tanner, C. M. (1991) *Neurol.* 41 (Suppl. 2), 89–91.
- Tucker, G. T. (1994) *J. Pharm. Pharmacol.* 46 (Suppl.), 417–424.
- Wolf, C. R. (1990) *Cancer Surv.* 9, 437–474.
- Yamazaki, H., Ueng, Y.-F., Shimada, T., & Guengerich, F. P. (1995) *Biochemistry* 34, 8380–8389.
- Zhao, Q., Smith, G., Modi, S., Paine, M., Wolf, C. R., Tew, D., Lian, L.-Y., Primrose, W. U., Roberts, G. C. K., & Driessen, H. P. C. (1996) *J. Struct. Biol.* 116, 320–325.

BI962633P